ASM Handbook, Volume 8: Mechanical Testing and Evaluation
H. Kuhn, D. Medlin, editors, p3–12
DOI: 10.31399/asm.hb.v08.a0003254

Introduction to the Mechanical Behavior of Metals

Todd M. Osman, U.S. Steel Research
Joseph D. Rigney, General Electric Aircraft Engines

THE SUCCESSFUL EMPLOYMENT OF METALS in engineering applications relies on the ability of the metal to meet design and service requirements and to be fabricated to the proper dimensions. The capability of a metal to meet these requirements is determined by the mechanical and physical properties of the metal. Physical properties are those typically measured by methods not requiring the application of an external mechanical force (or load). Typical examples of physical properties are density, magnetic properties (e.g., permeability), thermal conductivity and thermal diffusivity, electrical properties (e.g., resistivity), specific heat, and coefficient of thermal expansion. Mechanical properties, the primary focus of this Volume, are described as the relationship between forces (or stresses) acting on a material and the resistance of the material to deformation (i.e., strains) and fracture. This deformation, however, may or may not be evident in the metal after the applied load is removed. Different types of tests, which use an applied force, are employed to measure properties, such as elastic modulus, yield strength, elastic and plastic deformation (i.e., elongation), hardness, fatigue resistance, and fracture toughness. Typical specimens for these evaluations are shown in Fig. 1.

As will be highlighted throughout the discussion below, mechanical properties are highly dependent on microstructure (e.g., grain size, phase distribution, second phase content), crystal structure type (i.e., the arrangement of atoms), and elemental composition (e.g., alloying element content, impurity level). A common illustration of the relationship between microstructure and mechanical performance is the often observed increase in yield stress with a decrease in grain size. Relationships like these between metal structure and performance make mechanical property determination important for a wide variety of structural applications in metal working, in failure analysis and prevention, and in materials development for advanced applications.

The following discussions are designed to briefly introduce typical relationships between metallurgical features (such as crystal structures and microstructures) and the mechanical behavior of metals. Using basic examples, deformation and fracture mechanisms are introduced. Typical properties measured during mechanical testing are then related to these deformation mechanisms and the microstructures of metals.

Structure of Metals

At the most basic level, metallic materials (as well as many nonmetallic ones) are typically crystalline solids, although it is possible to produce amorphous metals (i.e., those with random atomic arrangement) in limited quantities. The basic building block of the crystal lattice is the unit cell, some examples of which are shown in Fig. 2(a) through (d). By repeating this arrangement in three dimensions, a crystal

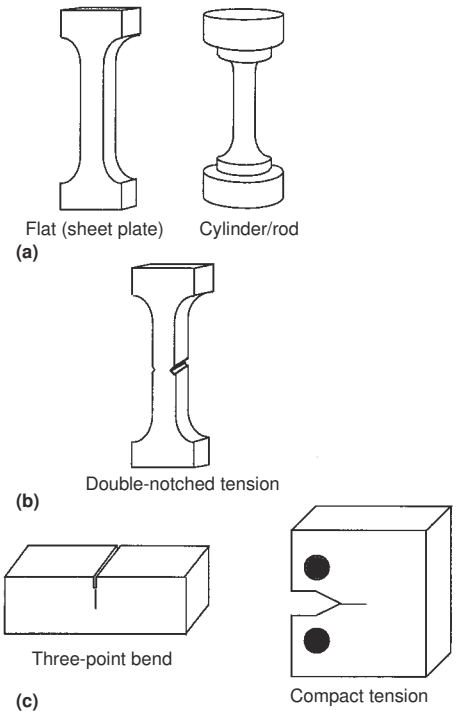

Fig. 1 Typical specimens for (a) tension testing, (b) notched tension testing, and (c) fracture toughness testing

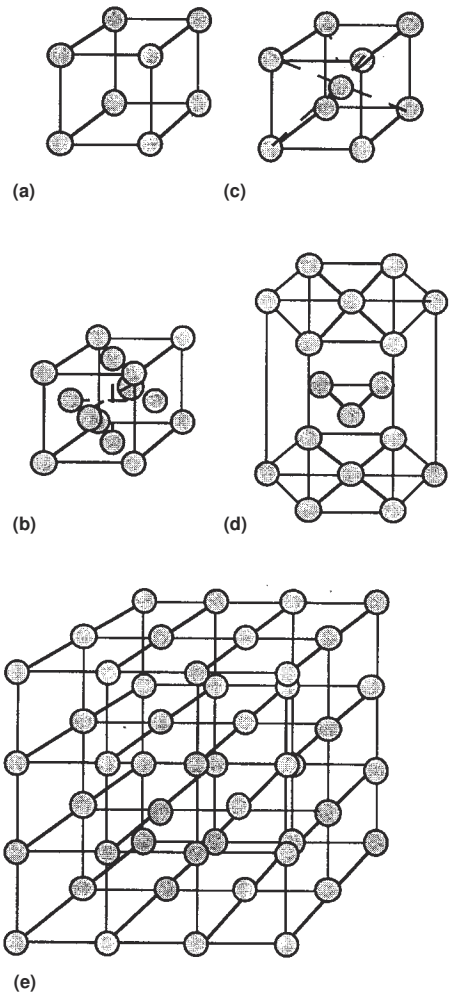

Fig. 2 Examples of crystal structures. Unit cells: (a) simple cubic, (b) face-centered cubic, (c) body- centered cubic, and (d) hexagonal close-packed. A crystal lattice: (e) three-dimensional simple cubic

lattice is formed (see Fig. 2e). Although the arrangement of atoms in space can be of fourteen different types (or Bravais lattices), most metals have face-centered cubic (fcc) (e.g., nickel, aluminum, copper, lead), body-centered cubic (bcc) (e.g., iron, niobium, tungsten, molybdenum), or hexagonal close-packed (hcp) (e.g., titanium, magnesium, zinc) structures as the unit cell structure. In very specific applications, materials can be used as single crystals where an entire component is fabricated with one spatial orientation repeating throughout. More often than not, however, engineering materials usually contain many crystals, or grains, as shown in Fig. 3(a) and (b). Depending on the composition and thermomechanical processing, these grains are typically approximately 1 to 1000 μm in size (although finer grain sizes can be produced via other techniques). While the crystal lattice within a grain is consistent, the crystalline orientations vary from one grain to another.

Although some nonstructural applications may require pure metals because of certain physical property advantages, additions of alloying elements are usually made for purposes of enhancing the mechanical properties or other material characteristics (e.g., corrosion resistance). Metal alloys may consist of over ten different elements in specific concentrations with the purpose to optimize a variety of properties. Minor alloying additions typically do not alter the basic crystal structure as long as the elements remain in solid solution. At sufficiently high concentrations, other phases (either with the same or different crystallographic forms) may precipitate within the base metal (at grain boundaries or in the grain interior) as shown in Fig. 3(c). Phase diagrams are used by metallurgists and materials engineers to understand equilibrium solubility limits in engineering alloys and predict the phases which may form during thermomechanical processing (Ref 2). As will be discussed later, solid solution elements and precipitates/particles are often used

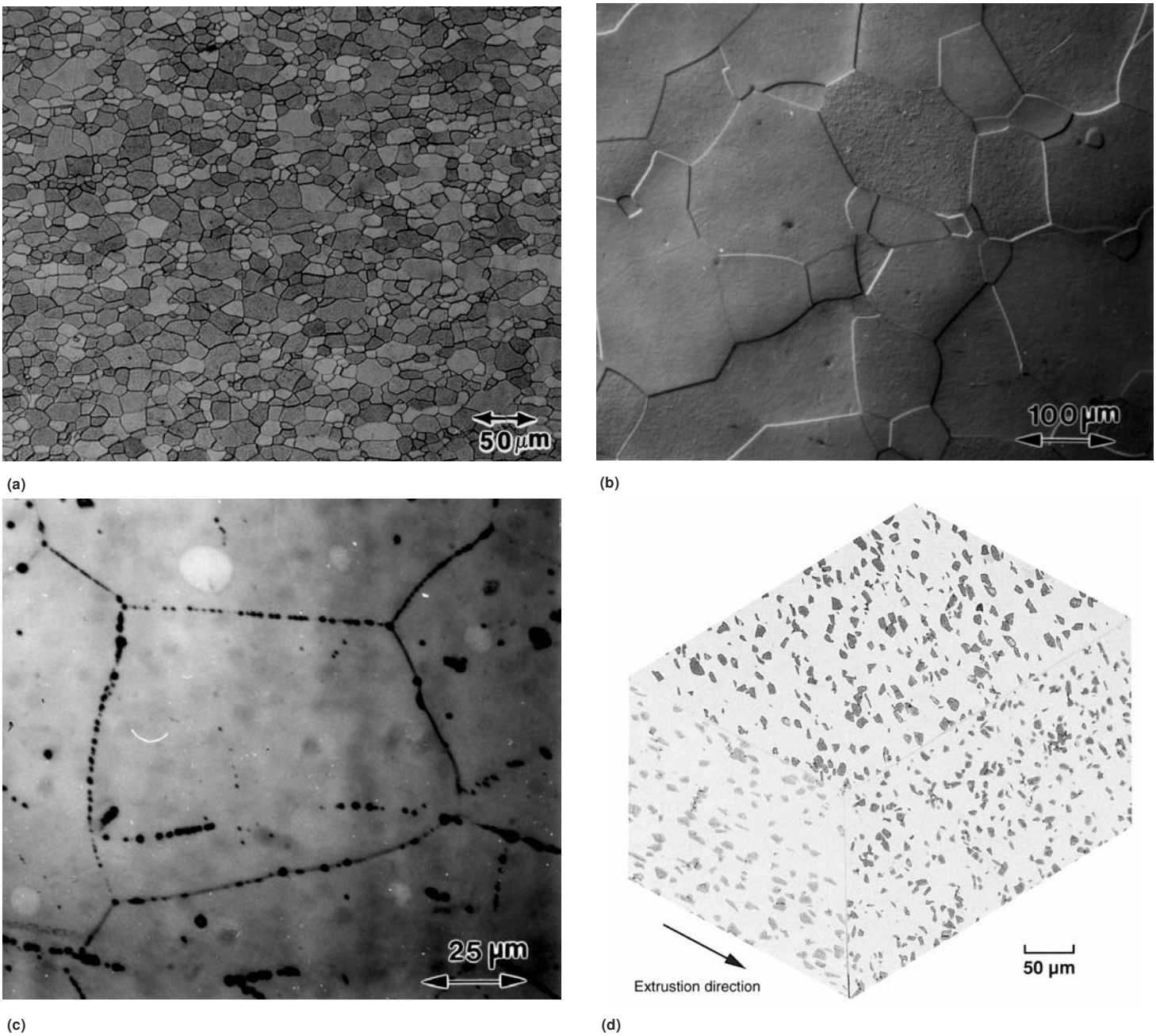

Fig. 3 Examples of metallic microstructures: (a) Grains in an ultralow-carbon steel. Courtesy of U.S. Steel. (b) Grains in pure niobium. (c) Precipitates at grain boundaries in niobium. (d) Discontinuously reinforced metal matrix composite (silicon carbide particles in an aluminum matrix). Source: Ref 1. Note: the grains in a–c are highlighted through the use of a chemical etchant.

during alloy design to improve the strength of a metal.

Metal matrix composites can also be fabricated in which dissimilar constituents (e.g., ceramics and intermetallics) are incorporated into the metallic microstructure in order to enhance mechanical properties. The example microstructure in Fig. 3(d) shows the reinforcement material to be dispersed throughout a continuous metallic matrix with the metal representing 50% or greater of the total volume. Although the example shows particles as the reinforcement, these materials can be designed with whiskers, short fibers, or long fibers (e.g., rods or filaments). Processing of these composites typically entails the incorporation of the reinforcement material into the metal using ingot metallurgy or powder metallurgy techniques (Ref 3).

To the structural engineer, or in the macroscopic view (1×), most metals appear to be continuous, homogeneous, and isotropic. Continuity assumes that structures do not contain voids; homogeneity assumes that the microstructure (in views at ~100–1000×) and properties will be identical in all locations; isotropic behavior assumes that the properties are identical in all orientations. While these assumptions have been used in continuum mechanics to study the strength of materials and structures under load, engineering materials are often inhomogeneous and anisotropic. While it is desirable to minimize such inhomogeneities, it is often impossible to completely eliminate them. As discussed above, microstructural evaluation typically shows that materials are comprised of an aggregate of grains of unique crystal structure and usually have second phases (with different properties) dispersed throughout the parent structure. Typically, materials will have variations in grain size, second phase size and distribution, and chemical composition, especially in binary and higher-order alloys. Fabrication route may also play a key role in affecting the preferred crystallographic orientation (or texture) of the grains, further contributing to the inhomogeneity and anisotropy of the microstructure. As will be shown later, all of these microstructural features can greatly influence the properties measured during mechanical testing.

When metals are subject to an external force, the response will depend on a number of factors. The type of loading (e.g., tension, compression, shear, or combinations thereof) is one key factor. The strain rate, temperature, nature of loading (monotonic versus alternating fatigue stresses), and presence of notches will also affect the deformation response of the metal. Chemical influences, such as those associated with stress-corrosion cracking (SCC) and hydrogen embrittlement, as well as physical alterations, such as those resulting from radiation damage, may affect the deformation behavior. Finally, the specimen size and surface preparation can influence the response observed during mechanical testing.

All of these factors are important and will be covered in various articles contained within this Volume. For simplicity, the remainder of this section focuses on basic examples to illustrate the relationship between the structure of a metal and the properties measured during mechanical testing.

Deformation of Metals

The basic principles of deformation and fracture can be described through the use of a uniaxial tension (or tensile) test. A detailed review of tension testing is presented later in this Volume; therefore, only a brief description is presented for the purpose of introducing deformation and fracture mechanisms in metals. In general, tensile tests are performed on cylindrical specimens (e.g., rods) or parallel-piped specimens (e.g., sheet and plate) as shown in Fig. 1(a). The samples are loaded uniaxially, along the length of the specimen. The applied load and extension (or change in length) of the sample are simultaneously measured.

The load and displacement are used to calculate engineering stress (s) and engineering strain (e) using Eq 1 and 2:

$$S = P/A_0 \quad \text{(Eq 1)}$$

$$e = \Delta L/L_0 = (L_i - L_0)/L_0 \quad \text{(Eq 2)}$$

where P is the applied load, L_0 is the initial gage length, L_i is the instantaneous gage length, A_0 is the initial gage cross-sectional area, and ΔL is the change in length. This analysis facilitates the comparison of results obtained when testing samples that differ in thickness or geometry. (For validity, the samples need to conform to certain design specifications as detailed later in this Volume.) Although these engineering values are adequate, the best measures of the response of a material to loading are the true stress (σ) and true strain (ε) determined by the instantaneous dimensions of the tensile specimen in Eq 3 and 4:

$$\sigma = P/A_i = S(1 + e) \quad \text{(Eq 3)}$$

$$\varepsilon = \ln (L_i/L_0) = \ln (1 + e) \quad \text{(Eq 4)}$$

Because the instantaneous dimensions of the specimen are not typically measured, the true stress and true strain may be estimated using the engineering stress and engineering strain (see Eq 1 and 2). It is noted that these estimations are only valid during uniform elongation (see Fig. 4) and are not applicable throughout the entire deformation range.

Figure 4 depicts a typical engineering stress-versus-engineering strain curve produced in a uniaxial tension test. In the initial stages of deformation, generally stress varies linearly with the strain. In this region, all deformation is considered to be elastic because the sample will return to its original shape (i.e., dimensions) when the applied stress is removed. If, however, the sample is not unloaded and deformation continues, the stress-versus-strain curve becomes nonlinear. At this point, plastic deformation begins, causing a permanent elongation that will not be recovered after unloading of the specimen. The stress at which a permanent deformation occurs is called the elastic (or proportional) limit; however, an offset yield strength (e.g., 0.2% offset) is typically used to quantify the onset of plastic deformation due to the ease and standardization of measurement. The tensile yield strength of most alloys is on the order of 10^2 to 10^3 MPa:

- 135 to 480 MPa (20–70 ksi) for low-carbon steels
- 200 to 480 MPa (30–70 ksi) for aluminum alloys
- 1200 to 1650 MPa (175–240 ksi) for high-strength steels

To understand the different deformation modes, the structure of a metal must be considered. Elastic deformation can be conceptualized by considering the bonds between individual atoms to be springs. As mentioned above, a metal will stretch under the application of a load, but will return to its original shape after the removal of that load if only elastic deformation occurs. Just as a spring constant relates the force to the applied displacement (i.e., $F = kx$), the elastic modulus (E) relates the tensile stress to the applied tensile strain (i.e., $\sigma = E\varepsilon$) and is simply the slope of the linear portion of the tensile stress-versus-tensile strain curve produced in the tension test. Differences in the measured elastic moduli for different metals can therefore be rationalized in part by the differences in the atomic bonds between the individual atoms within the crystal lattice.

Plastic deformation results in a permanent change of shape, meaning that after the load is removed, the metal will not return to its original dimensions. This implies a permanent displacement of atoms within the crystal lattice. If a perfect crystal is assumed, this deformation could only occur by breaking all of the bonds at

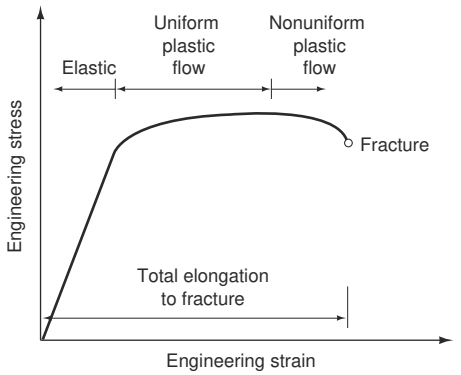

Fig. 4 Typical engineering stress-versus-engineering strain curve

once between two planes of atoms and then sliding one row (or plane) of atoms over another. Based on calculations using the theoretical bond strengths, this process would result in yield strengths on the order of 10^4 to 10^5 MPa. These strengths are much greater than those typically observed in actual metals (10^2 MPa); therefore, deformation must occur via a different method.

Even under the most ideal crystal growth conditions, metals are not crystallographically perfect, as shown in Fig. 2. Instead, the lattice may contain many imperfections. One such imperfection is an edge dislocation, which, for simple cubic structures, can be considered to be the extra half plane of atoms shown schematically in Fig. 5. Regions surrounding the dislocation may be a perfect array of atoms; however, the core of the dislocation is shown as a localized distortion of the crystal lattice. While it may appear that this structure is unfavorable, dislocations are necessary in metals. For example, at grain boundaries, dislocations are "geometrically necessary" to allow the individual grains of different orientations to match.

The nature and quantity of the dislocations become an integral aspect of plastic deformation. There are two generic types of dislocations, edge and screw, which are primarily differentiated by the manner in which each may traverse through the metallic crystal (Ref 4). It is noted that dislocations of mixed character (i.e., partially edge and partially screw) are most commonly observed. In general, both types of dislocations entail the stepwise movement of the dislocation across the crystal lattice as opposed to the displacement of an entire plane over another. This means that only one set of bonds is broken at a time as opposed to an entire plane. Motion now occurs on a distinct set of slip systems, which are combinations of planes—denoted as {uvw} or (uvw)—and directions—denoted as ⟨hkl⟩ or [hkl]—based on the closest packing of atoms within the crystal structure (see Fig. 6 for an example of crystallographic planes and directions) (Ref 5). For example, motion will predominantly occur on {111}⟨110⟩ slip systems in fcc metals and on {110}⟨111⟩, {112}⟨111⟩, or {123}⟨111⟩ slip systems in bcc metals. As a result, differences in the plastic behavior of a given type of metal (e.g., aluminum-killed versus fully stabilized steels) can in part be rationalized by which slip systems are active during deformation. Likewise, differences in the properties between different metal types (e.g., bcc iron versus fcc aluminum versus hcp titanium) can be related to the active slip systems in each metal and the relative ease with which dislocations can move within the slip systems.

Motion within a slip system is governed by the critical resolved shear strength (τ_{CRSS}). As shown schematically in Fig. 7 for a single crystal, the attainment of τ_{CRSS} on a given slip system is related to the geometric relationship between the applied load and the slip system. This relationship is described mathematically by Schmid's law.

In polycrystalline metals, plastic flow typically does not occur at a constant stress. In contrast, an increased stress must be applied to produce additional deformation, as shown in Fig. 4. This trend can be rationalized by considering the motion, interaction, and multiplication of dislocations. As plastic flow continues, the number of dislocations increases, typically in a parabolic fashion (Ref 6). These dislocations begin to interact with each other and with interfaces such as grain boundaries. When a dislocation encounters a grain boundary, motion is usually halted. Although direct transmission to the neighboring grain may occur (Ref 7–9), more typically dislocations start to build up at the grain boundary and dislocation tangles may be created. As this buildup continues, a back stress develops that opposes the motion of additional dislocations, giving rise to work hardening (i.e., the increase in strength with straining shown in Fig. 4) (Ref 7).

Typically, the work hardening of a metal is calculated by assuming a parabolic fit to the true stress-versus-true strain data as suggested by Eq 5:

$$\sigma = K\varepsilon^n \qquad \text{(Eq 5)}$$

where K is the strength coefficient and n is the strain-hardening exponent. The true stress and true strain measured (or calculated from Eq 1–4) can be used to determine the strain-hardening exponent (n-value). This exponent is simply the slope calculated after plotting the logarithm of true stress versus the logarithm of true strain:

$$\log \sigma = n \log \varepsilon + \log K \qquad \text{(Eq 6)}$$

As will be discussed later in this Volume, the value of the strain-hardening exponent becomes important when predicting the response of metals to straining during primary metalworking as well as forming operations for final components.

As shown in Fig. 4, there is a point in the stress-versus-strain curve where the work hardening can no longer compensate for the increase in local stress arising from the reduced cross-sectional area. At this point, nonuniform plastic flow occurs in which deformation is concentrated in one region, called a neck. Necking in the tensile specimen usually coincides with the maximum stress (i.e., the ultimate tensile strength) in an engineering stress-versus-engineering strain curve.

Figure 7 introduces the influence of crystallographic orientation on the deformation of single crystals. Although this relationship becomes more complex in polycrystalline metals, the deformation will still depend on the orientation of the load with respect to the active slip systems. For example, the tensile properties of a highly oriented (i.e., textured anisotropic) metallic sheet product will be different when measured parallel (longitudinal), normal (trans-

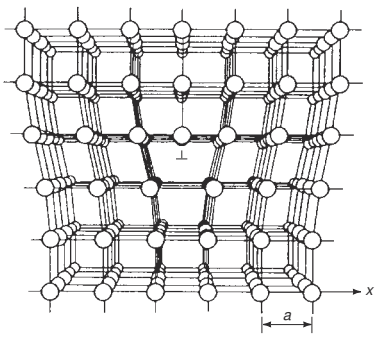

Fig. 5 Schematic of an edge dislocation

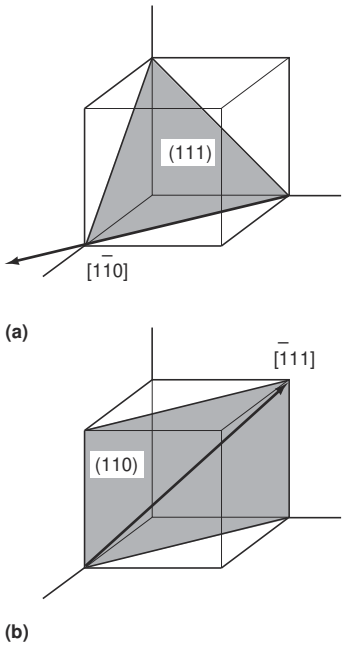

Fig. 6 Examples of crystallographic planes and directions. (a) (111) [1 $\bar{1}$ 0] and (b) (110) ($\bar{1}$ 1 1)

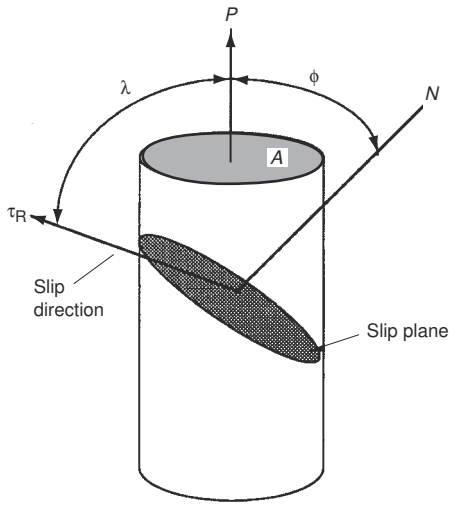

Fig. 7 Schmid's law. $\tau_R = (P/A) \cos \phi \cos \lambda$. Note: plastic flow on a given slip system will initiate when $\tau_R > \tau_{CRSS}$

verse), or at 45° (diagonal) to the rolling direction. The variation in plastic deformation in different orientations can be defined in terms of Lankford values (Ref 10). The individual Lankford values in Eq 7 are calculated using strains measured in a tensile test:

$$r = \varepsilon_w/\varepsilon_t = -\varepsilon_w/(\varepsilon_l + \varepsilon_w) \quad \text{(Eq 7)}$$

where ε_w, ε_t, and ε_l are width, thickness, and longitudinal true strains measured from a parallel-sided tensile specimen, respectively. The mean plastic anisotropy (r_m) and normal plastic anisotropy (Δr) can be calculated using Eq 8 and 9, respectively:

$$r_m = \frac{(r_0 + 2r_{45} + r_{90})}{4} \quad \text{(Eq 8)}$$

$$\Delta r = \frac{(r_0 - 2r_{45} + r_{90})}{2} \quad \text{(Eq 9)}$$

where r_0, r_{45}, and r_{90} are the r-values calculated from sheet tensile specimens oriented at 0° (parallel), 45° (diagonal), and 90° (normal) to the rolling direction, respectively. As may be expected, Lankford values depend on the crystal structure. Figure 8 relates the calculated Lankford values with crystallographic texture for a low-carbon steel as measured using X-ray diffraction techniques, further highlighting the influence of metallic structure on mechanical behavior.

Strength of Metals

Thus far, the mechanical properties of crystalline metals have been discussed only in relationship to the crystal lattice. Because most metals are comprised of many grains (see Fig. 2), properties such as yield strength and ductility (i.e., elongation to fracture) are also highly dependent on the microstructure. Once again, the influence of both of these factors can be rationalized by considering the motion of dislocations. The strength of a metal is related to the ease, or conversely the difficulty, of dislocation motion. If dislocation motion is uninhibited (i.e., motion is initiated easily and continues without hindrance), the strength will be low and relatively little work hardening will occur. In contrast, the presence of obstacles, or barriers, within the microstructure slow dislocation motion, resulting in an increase in strength.

Grain boundaries provide an obstacle to dislocation motion. As the grain size is decreased, the strength (σ) of the metal typically increases according to the Hall-Petch relationship given in Eq 10 and illustrated in Fig. 9 (Ref 12, 13):

$$\sigma = \sigma_0 + kd^{-1/2} \quad \text{(Eq 10)}$$

where σ_0 is the intrinsic strength of the metal, k is a coefficient, and d is the grain diameter. At small grain sizes, there is a larger probability of dislocation-dislocation interactions (e.g., dislocation "pile-up" at the grain boundaries), leading to a larger resistance to dislocation motion. As the grain size increases, the opposition to dislocation motion, due to back stresses associated with dislocation tangles at grain boundaries, lessens due to the larger distances between grain boundaries. Therefore, the lower strength of a large-grained metal when compared to a small-grained metal can be rationalized by a decrease in the resistance to dislocation motion.

The strength of a metal will also be related to the impurity content. Sometimes elements are intentionally added to metals, such as adding nickel to copper or phosphorus to steel. Other times, the presence of impurities, such as inclusions (e.g., oxides) in copper or solute carbon in steel, may be undesired. In order to rationalize these statements, the effect of each on plastic flow in metals needs to be considered. Figure 10 schematically illustrates two scenarios for incorporating atoms into a metallic matrix. Substitutional atoms (see Fig. 10a) take the place of matrix atoms. Because of the mismatch in atomic size between the substitutional atom and the matrix atom, the lattice may become locally strained. This lattice strain may impede dislocation motion and is conventionally considered to be the source of solid solution strengthening in metals. In general, the strengthening increment varies proportionally with the mismatch in atomic size and properties (specifically modulus) between the solute and solvent atoms, as shown in Fig. 11 (Ref 14).

Interstitial atoms can also be present within the metal (see Fig. 10b). In this case, the atom is much smaller than the matrix atoms and is located in the gaps (or interstices) in the crystal lattice. Most often, interstitial atoms can diffuse to the dislocation core (see Fig. 5) due to

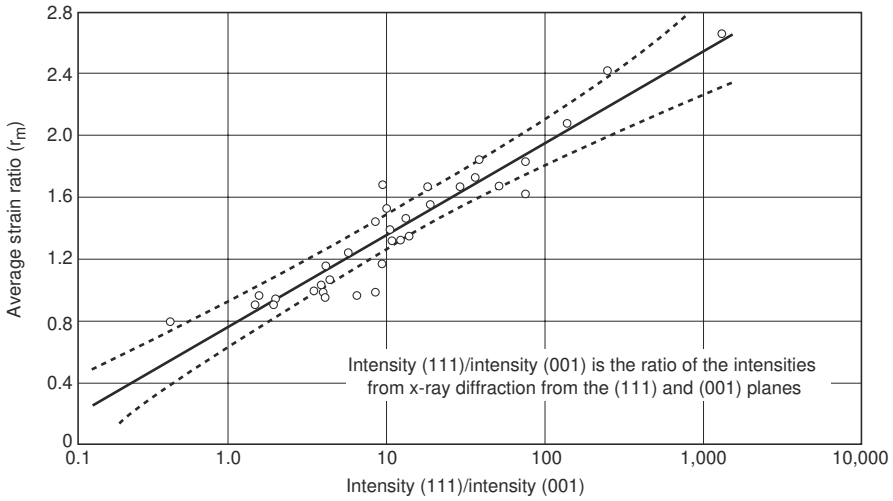

Fig. 8 Relationship between average (mean) plastic strain ratio (r_m) and crystallographic texture. Source: Ref 11

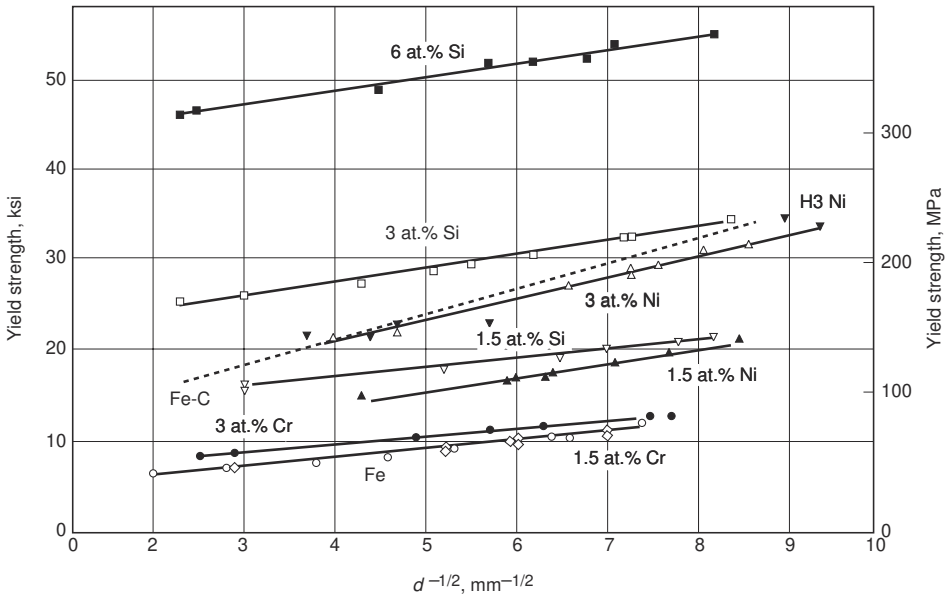

Fig. 9 Influence of grain size diameter (d) on yield strength for α-iron alloys. Source: Ref 12

the more open structure and the local tensile stresses in this region of the crystal lattice. The presence of the interstitial can inhibit dislocation motion, leading to dislocation "locking." This locking necessitates larger applied stresses to produce dislocation motion and further plastic deformation (Ref 15). In the classic example of carbon in iron, such a mechanism can result in discontinuous yielding as shown in Fig. 12. Deformation is not continuous, and a sharp upper yield point is typically observed followed by yielding at a constant stress. The serrations in the stress-versus-strain curve in Fig. 12 are most often attributed to the breakaway of dislocations from the solute carbon atoms. If the physical appearance of the tensile specimen is considered, localized distortions, called Lüders fronts (local regions of yielded material), will traverse the length of the specimen during yield-point elongation, and continuous plastic flow under an increasing load will not commence until the entire gage section has yielded. The extent of the yield-point elongation will depend on the density of mobile dislocations (i.e., those which are not "locked") and the ease with which these dislocations can move once initiated (Ref 16).

Impurity atoms and interstitial alloy additions can often cause second phase particles or precipitates to be present in the structure. A fine dispersion of small particles generally produces a higher strength than a coarse dispersion of large particles, as suggested in Fig. 13. At each volume fraction, small particles (10 Å) produce a higher strength than large (100 Å) particles. The strengthening increase is related to two factors: (a) a higher probability of the mobile dislocation intersecting the particles due to the smaller interparticle spacing and (b) the higher fracture resistance of smaller particles. Conversely, as the size of the particles increases at a constant volume fraction, the interparticle spacing increases, causing the particles to become less effective strengtheners (i.e., barriers to dislocation motion) (Ref 18). This effect can be observed in hot-rolled, low-carbon steels. At low coiling temperatures, finer carbides (e.g., Fe_3C and NbC) are typically produced, resulting in increased strength. At higher coiling temperatures, the carbide particles coarsen at a constant volume fraction, which typically results in a lower strength.

A similar scenario occurs with age-hardenable aluminum alloys. The strength of these alloys varies as a function of time at temperature as shown in Fig. 14. The yield strength initially increases proportionally with time, but eventually reaches a maximum. Longer aging times then result in decreased yield strength. These trends are once again directly related to the mechanisms of particle hardening. At short aging times, small coherent precipitates form that

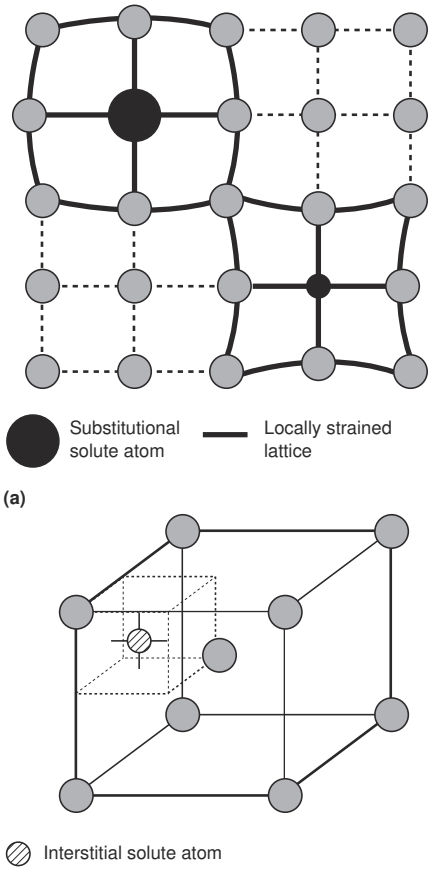

Fig. 10 Two scenarios of incorporating atoms into a metal matrix. (a) Substitutional atoms and (b) an interstitial atom in a body-centered cubic unit cell

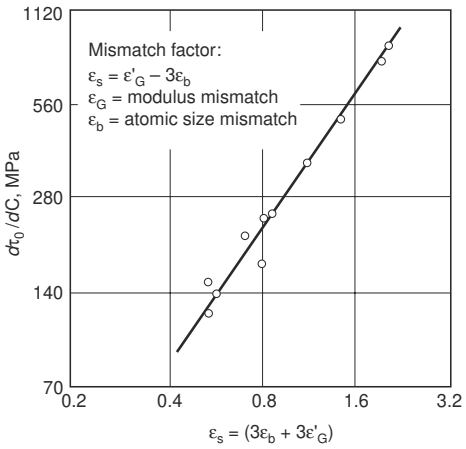

Fig. 11 Relationship between mismatch factor and strengthening increment ($\Delta\tau_0/\Delta C$) for solute atoms in copper alloys. Source: Ref 14

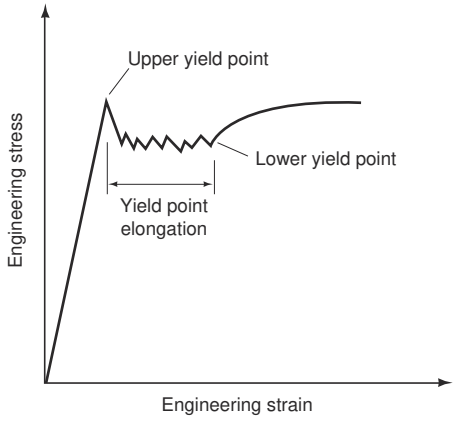

Fig. 12 Discontinuous yielding

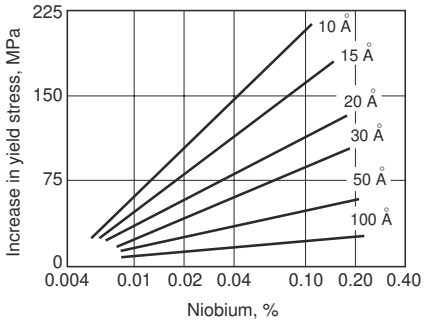

Fig. 13 Influence of particle size on yield strength (NbC in an HSLA steel). Source: Ref 17

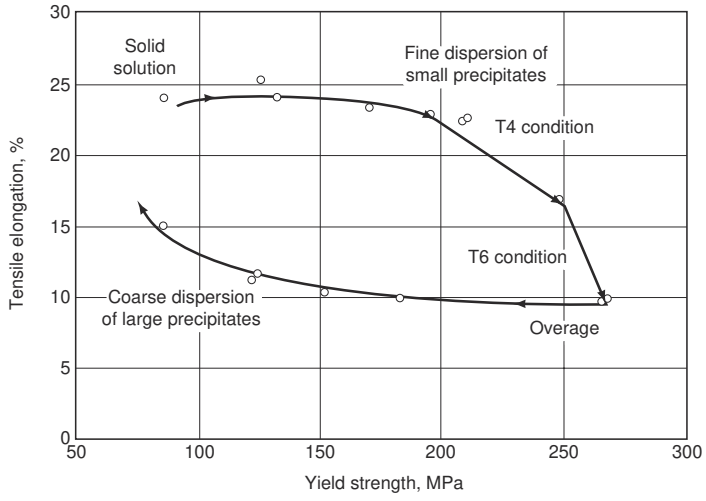

Fig. 14 Effect of aging heat treatment on ductility for a 2036 aluminum alloy. Source: Ref 19

are effective strengtheners. Overaging (i.e., soaking past the maximum yield strength) causes the particles to coarsen, and the interparticle spacing increases, resulting in the decreased strength.

Figure 14 also provides evidence that the ductility (i.e., the elongation prior to failure) of a metal will also be influenced by microstructural changes. Typically, there is an inverse relationship between strength and ductility. In order to rationalize this observation, the failure modes for metals need to be considered. In general, failure is classified as either ductile or brittle. There are many ways to differentiate the two types of failures, as illustrated in Table 1 and Fig. 15.

Ductile fracture is generally preceded by stresses that exceed the yield stress, and specimens failing with high reductions of area and by shear or microvoid coalescence. The process of ductile fracture by microvoid coalescence has been described by several authors (Ref 21–23). Microvoids nucleate predominantly at particles (e.g., inclusions, precipitates) that are present in nearly all metals. The particle size and shape, the particle-matrix interfacial strength, and the matrix flow strength influence the mechanism of void formation. In general, void nucleation by particle cracking is favored by increasing particle size, higher interfacial strengths, and the presence of nonequiaxed particles. By contrast, void nucleation by interfacial decohesion is more likely with smaller particles, weaker interfaces, and lower matrix flow strength (Ref 23). After nucleation, the voids will grow in the direction of the applied tensile stress and secondary voids can also nucleate at smaller particles. During necking, expansion of the voids can occur, leading to coalescence by void impingement (resulting in higher uniform strain) or by void sheet formation (lower, more local strain). After failure, a "dimpled" fracture surface is typically observed, as shown in Fig. 15(a).

As a result, the ductility of a metal typically decreases with increasing particle content, as shown in Fig. 16. An increase in particle volume fraction results in a larger number of potential void nucleation sites. Furthermore, there is an increased probability for the linkage of neighboring voids (impingement).

According to the descriptions in Table 1, brittle behavior is generally classified by failure at stresses below the yield strength and low reductions in area (little uniform strain) (Ref 25). Although this fracture process may be initiated by some dislocation activity, the levels generally detected are far below those found in a material exhibiting ductile behavior. Cleavage fracture, one of the brittle fracture modes, is distinguished by separation of individual grains along low index crystallographic planes in a transgranular manner—for example, iron cleaves along (100) planes. As shown in Fig. 15(b), lines on the cleavage facets, as seen in the scanning electron microscope (SEM), provide postmortem evidence of the direction of crack growth (i.e., the lines trace back to the origin of the failure

Table 1 Distinguishing characteristics of brittle versus ductile behavior depending on the scale of observation

Scale of observation	Brittle	Ductile
Structural engineer	Applied stress at failure is less than the yield stress	Applied stress at failure is greater than the yield stress
By eye (1×)	No necking, shiny facets, crystalline, granular	Necked, fibrous, woody
Macroscale (<50×)	"Low" RA or ductility	Medium to high RA
Microscale, scanning electron microscopy (100–10,000×)	Brittle microprocess, cleavage (see Fig. 15b), intergranular (see Fig. 15c)	Ductile microprocess, microvoid coalescence (see Fig. 15a)
Transmission electron microscopy (>10,000×)	May have a large level of local plasticity	High amount of plasticity globally

RA, reduction of area

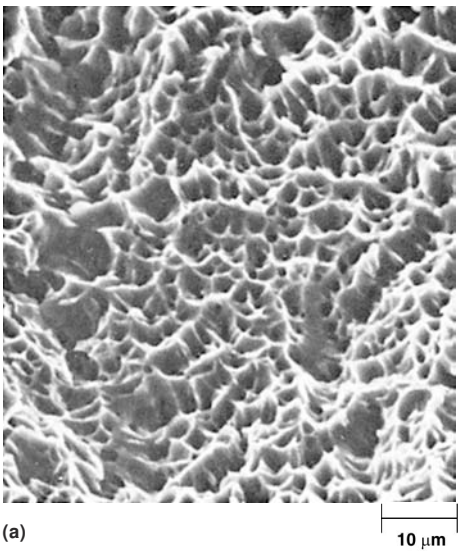

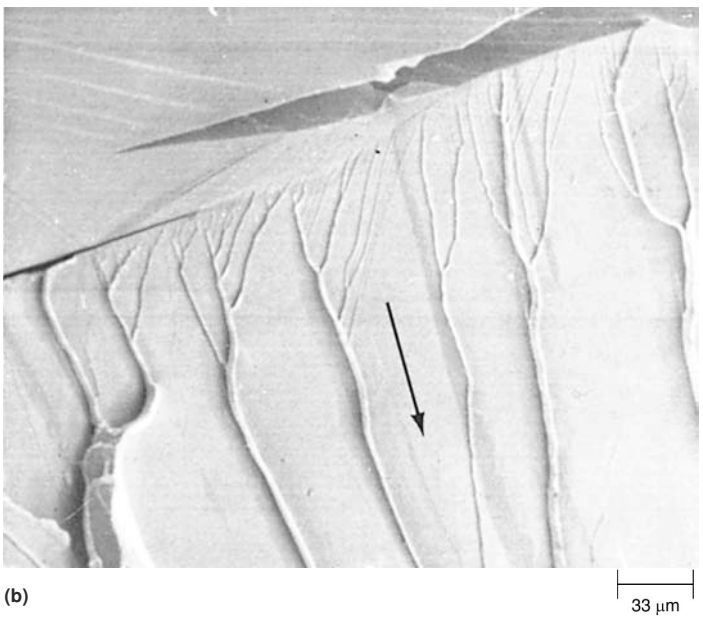

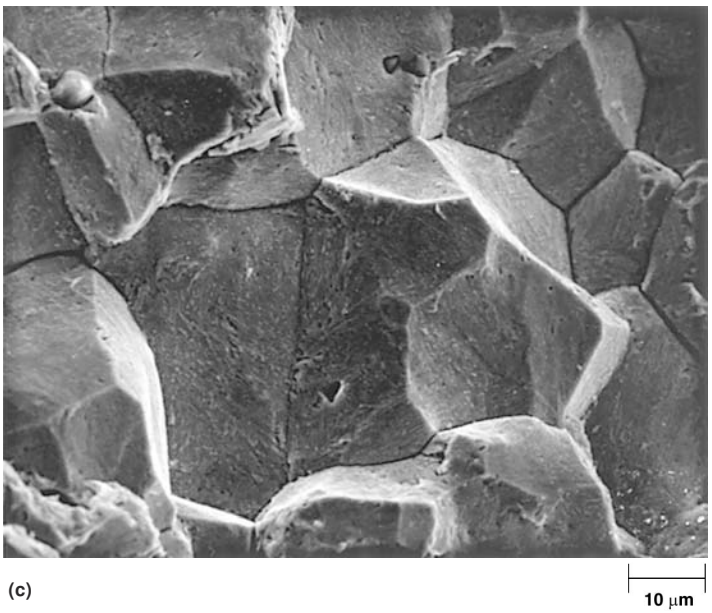

Fig. 15 Examples of fracture surfaces of metals failing by (a) microvoid coalescence, (b) cleavage, and (c) intergranular fracture. Source: Ref 20

origin). Each "line" is actually a step created between fractures propagating along parallel low index planes but separated by a small step. For pure cleavage, a step created on each side of the fracture surface should fit together except for some discrepancy that may occur due to some plasticity at the step. Another brittle fracture mode is intergranular fracture. In this case, a crack is initiated at grain boundaries and propagates along them. The grain-boundary facets appear to be "glassy smooth" as in Fig. 15(c). There may be evidence of local plasticity with tearing evident at the grain-boundary corners. It should be noted that intergranular microvoid coalescence, which is locally ductile fracture in grain boundary regions, can also occur.

Special Conditions in Flow: Temperature and Strain Rate

Many of the most widely employed structural metals have bcc lattices (e.g., steels, refractory metals) or fcc lattices (e.g., aluminum, copper). The strength of fcc metals is relatively insensitive to test temperature; however, the properties of bcc metals are typically highly dependent on testing conditions. This dissimilar behavior is related to the nature of dislocation motion with the individual crystal lattices. Face-centered cubic metals are more closely "packed" (i.e., a shorter distance exists between atoms in the unit cell of Fig. 2) than body-centered cubic metals. A common slip system (i.e., $\{111\}\langle 110\rangle$) prevails across temperature regimes for fcc metals; however, dislocations have been found to move on different slip systems in bcc metals (e.g., $\{110\}\langle 111\rangle$, $\{112\}\langle 111\rangle$, or $\{123\}\langle 111\rangle$ for α-iron), depending on temperature (Ref 5, 25, 26).

In bcc metals, a substantial increase in flow stress (or strength) can be observed at temperatures less than one-fifth the melting temperature of the metal. Under these conditions, the internal resistance to dislocation motion can greatly increase. If the barriers to dislocation motion are considered further, they can be separated into athermal (i.e., not influenced by temperature) and thermal (i.e., dependent upon temperature) components (Ref 5). Athermal barriers, such as long-range interaction of dislocations, are too large to be overcome by gliding dislocations utilizing only thermal fluctuations and the applied stress to move from one site to another. In contrast, thermal barriers, such as solute atoms and precipitates, are surmountable by dislocations with the assistance of this thermal energy and an applied stress.

At low temperatures, the thermal activation of dislocations is minimal; therefore, a large applied stress is required for deformation. At higher temperatures, thermal activation will assist in dislocation motion "around" the thermal barriers. The applied stress necessary for plastic flow is lowered, which reduces the measured strength. Above a critical temperature, thermal activation provides a substantial portion of the driving force for dislocation motion, such that the strength of the material will be primarily determined by athermal barriers.

The previous discussion assumes that plastic flow will take place and that there is a constancy of fracture mechanism. Such an assumption is not necessarily valid for bcc metals. These metals show a transition in fracture mode from ductile (microvoid coalescence or shear) to brittle (e.g., cleavage) with decreasing temperature. This transition can be conceptualized using a simple Orowan-type construction (Ref 27) such as the one shown in Fig. 17. The brittle fracture stress (the cleavage stress) varies weakly with temperature and may be considered to be approximately independent of temperature. The yield strength, however, will increase with decreasing temperatures as discussed previously. The temperature where the two curves intersect (T1 in Fig. 17) is considered to be the ductile-to-brittle transition temperature (DBTT) for the metal. Above this temperature, the metal will yield prior to fracture, while below the DBTT, cleavage occurs without macroscopic yielding.

In addition to temperature, the rate of loading (i.e., strain rate) during testing will also greatly affect the measured mechanical properties of bcc metals. In general, an increase in strain rate is analogous to a decrease in temperature. The combined effect of strain rate ($\dot{\varepsilon}$) and temperature (T) can be seen in Eq 11 (Ref 5):

$$\dot{\varepsilon} = \dot{\varepsilon}_0 \exp\left[\frac{-\Delta G^*(\tau^*)}{kT}\right] \qquad \text{(Eq 11)}$$

where ΔG^* is the Gibbs free energy associated with the shear stress (τ^*) required to overcome short-range obstacles and $\dot{\varepsilon}_0$ is the product of the mobile dislocation density, the vibration frequency for the dislocation segment, and the Burgers vector for the dislocation, the distance that the dislocation may "jump." This relationship illustrates that sufficiently high temperatures or low enough strain rates increase the probability for exciting dislocation motion through a thermal activation event in the presence of an applied load. On the other hand, low temperatures and high strain rates can lead to significant strengthening due to smaller contributions by thermal activation.

For bcc metals, which exhibit a ductile-to-brittle transition, increasing the strain rate can have an additional effect. As discussed previously and shown schematically in Fig. 17, the yield strength increases at a higher strain rate. This shifts the temperature dependence of yield strength, resulting in an intersection with the brittle fracture stress at a higher temperature (T2 in Fig. 17). The end result is that the measured DBTT will be greater at a higher strain rate (T2) than at a lower strain rate (T1).

Special Conditions in Fracture: Notches and Cracks

The deformations and processes governing fracture in metals are affected by both the stresses and strains experienced in the specimen. In a simple tension test, the stresses are designed to be uniform throughout the cross section of the sample. When stress is applied to a component with a notch, crack, or other stress concentration, regions in the vicinity of these features will always experience much higher stresses compared to unaffected regions, and the strains produced can be very different from what would be predicted by the stresses. The stress fields created around stress concentrations are controlled by three factors: (a) the extent of deformation prior to failure, (b) the mode of loading (i.e., the relative orientation of the applied load with respect to the plane of the crack), and (c) the constraints, if any, on the cracked body (Ref 25, 27).

As a result, the mechanical properties measured when testing specimens with notches (see Fig. 1b) or cracks (see Fig. 1c) will be much different than those observed in uniaxial tension tests. For the case of notched tensile specimens, the measured tensile yield strength often will be greater than that observed in a uniaxial tension test. However, the ductility and load-carrying capacity will be decreased. As the sample is loaded, the notched region

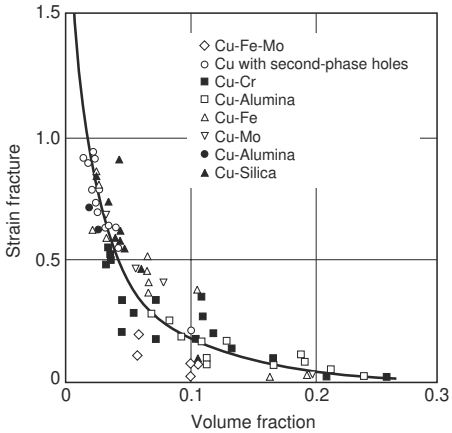

Fig. 16 Influence of particle content on ductility. Source: Ref 24

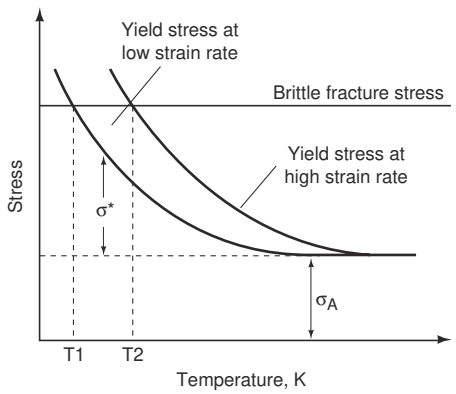

Fig. 17 Schematic illustration of the ductile-to-brittle transition in body-centered cubic metals

will yield first due to the elevated local stresses and strains associated with the notches. The maximum stress ahead of the notch will be a function of the geometry of the notch and the applied loading (Ref 28, 29). Furthermore, the stresses are no longer purely uniaxial (such as is developed in a tensile test), but now become triaxial (i.e., tensile stresses in the three primary directions of space). If ductile fracture via microvoid coalescence is reconsidered, the elevated stress and strain fields may accelerate the nucleation of secondary voids. The void growth rate will also increase proportionally to the level of the triaxial stresses, resulting in reduced ductility for notched samples compared to smooth, uniaxial tensile specimens (Ref 30, 31).

A more severe stress concentration will occur in cracked specimens, such as those used to determine fracture toughness (see Fig. 1c). In the most limiting case (e.g., opening of a sharp crack or Mode I loading), the component is highly constrained (with the level of constraint dependent on mechanical properties and component size). Under these conditions and with the application of a sufficient load, the peak tensile stresses around the crack tip can reach levels as high as five times the yield strength of the metal. As in the case of notched specimens, this change in stress state reduces the measured fracture strains due to a local acceleration of the fracture process.

To understand effects of cracks in ductile metals, the interactions between microstructural features and the elevated stress fields around the crack tip need to be considered. Ahead of a sharp crack, a finite volume of material is subjected to deformations at high stress values. To a first-order approximation, this volume of material, or the "plastic zone" in plane strain, can be represented as the radius of a circle as described by Eq 12 (Ref 25, 27):

$$r_p = \frac{1}{6\pi}\left(\frac{K_I}{\sigma_{ys}}\right)^2 \qquad \text{(Eq 12)}$$

where r_p is the distance from the crack to the elastic-plastic boundary, K_I is the stress intensity calculated from the geometry and loading conditions, and σ_{ys} is the uniaxial yield strength of the material. The highly constrained regions experiencing the triaxial stress state are located within this volume. As a result, the size of this zone relative to the microstructural features becomes a key factor influencing the measured properties of cracked specimens.

In general, the stresses are highest in a plastically deforming material ahead of the crack tip. In contrast, the plastic strains are highest at the notch tip and decrease after a critical distance, which is approximately equivalent to the crack-opening displacement (i.e., the relative displacement of the "mouth" of the crack) (Ref 27). The extent of the strained region often becomes comparable to microstructural features (grain size, interparticle particle spacing, etc.) and can initiate failure. When large strains are required for fracture, the crack-opening displacement must reach a critical size as to envelop the microstructural features responsible for void nucleation. Depending on the intrinsic fracture resistance of the metal, void growth and failure will occur when this zone becomes 1.0 to 2.7 times the microstructural feature responsible for fracture (e.g., the grain size or the mean spacing of second-phase particles) (Ref 32, 33).

An example of this type of fracture process can be seen in the case of metal matrix composites (i.e., a ductile metal matrix with brittle reinforcement particles). Crack growth in such a material is schematically shown in Fig. 18. When a crack in the ductile matrix is loaded, the large stresses ahead of the notch promote void nucleation by particle fracture or interface decohesion. This void nucleation limits the straining capacity of the metal in the vicinity of the crack tip. The high strain field ahead of the tip then allows for continued growth of the nucleated voids to the point of instability, as the blunted crack links with the microcrack. This process of microcracking, crack-tip blunting, and failure of the matrix (void formation) between the particles continues as the crack propagates. This mechanism gives cracks an easy path for failure and clearly shows that the presence of a stress raiser exacerbates the processes of fracture compared to the case of uniaxial tension.

The interaction between the microstructure of a metal and the resulting properties measured during mechanical testing is further illustrated by Fig. 18. In this example, crack propagation from a notch or crack tip is related to the spacing of microstructural features. As a result, a metal with a reduced volume fraction of particles (and the assumed increased interparticle spacing) can exhibit a greater resistance to fracture than a metal with a larger amount of particles (in agreement with Fig. 16).

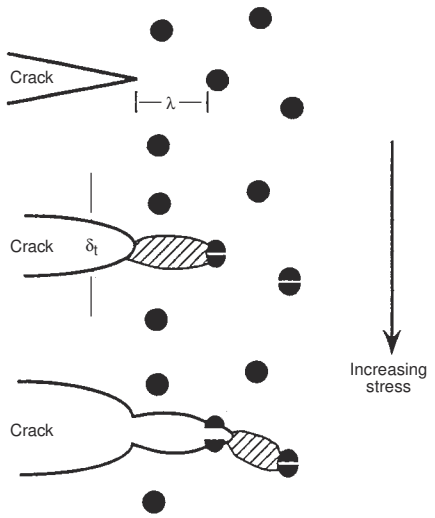

Fig. 18 Rice and Johnson model for failure in ductile matrix composites. Top: sharp crack blunts. Middle: particle cracking occurs followed by ductile tearing. Bottom: crack propagation. λ is the interparticle spacing; δ_t is the crack opening displacement. Source: Ref 32

Summary

The previous discussions were designed to provide a brief introduction to the influence of microstructure on the mechanical behavior of metals. The mechanisms of elastic and plastic flow have been highlighted along with the response of metals to stress raisers such as notches. The properties measured during mechanical testing can be rationalized by considering the effect of microstructural features, such as grain size and particle content, on deformation mechanisms. During quality-control testing, a larger-than-normal strength (or hardness) for a given metal during testing might be the result of grain refinement during processing. A lower strength observed for an age-hardenable metal might be the result of particle coarsening during overaging in heat treatment. Likewise, a dramatic drop in ductility might be the result of an increased inclusion content (or, in some cases, from embrittlement due to impurity segregation to the grain boundaries).

The relationship between microstructure and mechanical properties is also important when designing processing conditions, as well as in material selection for various applications. If increased strength in the final product is desired, solid-solution strengtheners may be added (e.g., adding nickel to copper), or the thermomechanical processing may be changed to produce a finer distribution of particles (e.g., lowering the coiling temperature for hot-rolled steel). If the final application has notches, it may be beneficial to use a metal with a lower inclusion content.

The remaining articles in this Volume will continue to build on this theme. In particular, the design of mechanical testing procedures and the analysis of resultant data will be highly dependent on the structure of the metal. Small variations in this structure may result in large changes in mechanical properties. As highlighted above, these changes are a direct consequence of the relationship between the metallurgical features and the mechanisms of deformation and fracture.

REFERENCES

1. T.M. Osman, J.J. Lewandowski, and W.H. Hunt, Jr., *Fabrication of Particulates Reinforced Metal Composites,* ASM International, 1990, p 209
2. Alloy Phase Diagrams, Vol 3, *ASM Handbook,* ASM International, 1992
3. D. Hull, *An Introduction to Composite Materials,* Cambridge University Press, 1975

4. R.W.K. Honeycombe, *The Plastic Deformation of Metals,* 2nd ed., Edward Arnold, London, 1984
5. D. Hull and D.J. Bacon, *Introduction to Dislocations,* Pergamon Press, London, 1984
6. A.S. Keh, *Direct Observations of Imperfections in Crystals,* J.B. Newbrick and J.H. Wernick, Ed., Interscience Publishers, New York, 1962, p 213–238
7. A.N. Stroh, *Proc. R. Soc.* (London), Vol 223, 1954, p 404
8. Z. Shen, R.H. Wagoner, and W.A.T. Clark, *Acta Metall.,* Vol 36, 1988, p 3231
9. T.C. Lee, I.M. Robertson, and H.K. Birnbaum, *Metall. Trans. A,* Vol 21, 1990, p 2437
10. W.T. Lankford, S.C. Snyder, and J.A. Bauscher, *Trans. ASM,* Vol 42, 1950, p 1197–1228
11. J.F. Held, *Proc. Mechanical Working and Steel Processing Conference,* Vol 4, AIME, New York, 1965, p 3
12. W.B. Morrison and W.C. Leslie, *Metall. Trans.,* Vol 4, 1973, p 379
13. N.J. Petch, *J. Iron Steel Inst. Jpn.,* Vol 173, 1953, p 25
14. Fleischer, *Acta Metall.,* Vol 11, 1963, p 203
15. J. Heslop and N.J. Petch, *Philos. Mag.,* Vol 2, 1958, p 649
16. G.T. Hahn, *Acta Metall.,* Vol 10, 1962, p 727
17. W.J. Murphy and R.G.B. Yeo, *Met. Prog.,* Sept 1969, p 85
18. J.W. Martin, *Micromechanisms in Particle Hardened Alloys,* Cambridge University Press, 1980
19. L.B. Morris et al., *Formability of Aluminum Sheet Alloys, Aluminum Transformation Technology and Applications,* C.A. Pampillo et al., Ed., American Society for Metals, 1982, p 549
20. V. Kerlins and A. Philips, Modes of Fracture, *Fractography,* Vol 12, ASM Handbook, ASM International, 1987, p 12–71
21. I. Kirman, *Metall. Trans.,* Vol 2, 1971, p 1761
22. R.H. Van Stone, T.B. Cox, J.R. Low, and J.A. Psioda, *Int. Met. Rev.,* Vol 30, 1985, p 157
23. W.M. Garrison, Jr. and N.R. Moody, *J. Phys. Chem. Solids,* Vol 48, 1987, p 1035
24. B.I. Edelson and W.M. Baldwin, *Trans. ASM,* Vol 55, 1962, p 230
25. G.E. Dieter, *Mechanical Metallurgy,* 3rd ed., McGraw-Hill, 1986
26. U.F. Kocks, A.S. Argon, and M.F. Ashby, *Thermodynamics of Slip,* Pergamon Press, New York, 1975
27. J.F. Knott, *Fundamentals of Fracture Mechanics,* Butterworths, London, 1981
28. D.J.F. Ewing and R. Hill, J. *Mech. Phys. Solids,* Vol 5, 1957, p 115
29. W.D. Pilkoy, *Peterson's Stress Concentration Factors,* 2nd ed., John Wiley & Sons, Inc., New York, 1997
30. J.R. Rice and D.M. Tracey, *J. Mech. Phys. Solids,* Vol 17, 1969, p 201
31. P.F. Thomason, *Ductile Fracture of Metals,* Pergamon Press, Oxford, 1990
32. J.R. Rice and M.A. Johnson, *Inelastic Behavior of Solids,* M.F. Kanninen, Ed., McGraw-Hill, New York, 1970, p 641
33. J. R. Rice, *Fracture—An Advanced Treatise,* H. Liebowitz, Ed., Academic Press, New York, 1968, p 191

SELECTED REFERENCES

Structure of Metals

- D.A. Porter and K.E. Easterling, *Phase Transformations in Metals and Alloys,* Van Nostrand Reinhold, Birkshire, UK, 1987
- C.R. Barrett, W.D. Nix, and A.S. Tetelman, *The Principles of Engineering Materials*, Prentice-Hall, Inc., Englewood Cliffs, New Jersey, 1973
- W. Hume-Rothery and G.V. Raynor, *The Structure of Metals and Alloys,* The Institute of Metals, London, 1956
- D. Hull and D.J. Bacon, *Introduction to Dislocations,* Pergamon Press, London, 1984
- P.B. Hirsch, Ed., Defects, Vol 2, *The Physics of Metals,* Cambridge University Press, Cambridge, 1975
- U.F. Kocks, C.N. Tome, and H.-R. Wenk, T*exture and Anisotropy,* Cambridge University Press, Cambridge, 1998
- D. Hull, *An Introduction to Composite Materials,* Cambridge University Press, 1975

Deformation of Metals and Strength of Metals

- M.A. Meyers and K.K. Chawla, *Mechanical Metallurgy: Principles and Applications,* Prentice Hall, Inc., 1984
- J.M. Gere and S.P. Timoshenko, *Mechanics of Materials,* 2nd ed., PWS Publishers, 1984
- T.H. Courtney, *Mechanical Behavior of Materials,* McGraw-Hill, New York, 1990
- J.W. Martin, *Micromechanisms in Particle Hardened Alloys,* Cambridge University Press, 1980
- P.F. Thomason, *Ductile Fracture of Metals*, Pergamon Press, Oxford, 1990
- R.W.K. Honeycombe, *The Plastic Deformation of Metals*, 2nd ed., Edward Arnold, London, 1984

Special Conditions in Flow and Fracture

- J.F. Knott, *Fundamentals of Fracture Mechanics,* Butterworths, 1981
- B.R. Lawn and T.R. Wilshaw, *Fracture of Brittle Solids,* Cambridge University Press, 1975
- H.L. Ewalds and R.J.H. Wanhill, *Fracture Mechanics,* Edward Arnold, London, 1985
- D. Broek, *Elementary Engineering Fracture Mechanics,* Martinus Nishoff Publishers, 4th ed., Dordrecht, Netherlands, 1987

ASM Handbook, Volume 8: Mechanical Testing and Evaluation
H. Kuhn, D. Medlin, editors, p13–25
DOI: 10.31399/asm.hb.v08.a0003255

Introduction to the Mechanical Behavior of Nonmetallic Materials

M.L. Weaver and M.E. Stevenson, The University of Alabama, Tuscaloosa

MANY DIFFERENT types of materials are used in applications where a resistance to mechanical loading is necessary. The type of material used depends strongly upon a number of factors including the type of loading that the material will experience and the environment in which the materials will be loaded. Collectively known as *engineering materials* (Ref 1), they can be pure elements, or they can be combinations of different elements (alloys and compounds), molecules (polymers), or phases and materials (composites). All solid materials are typified by the presence of definite bonds between component atoms or molecules. Ultimately, it is the type of bonding present that imparts each class of materials with distinct microstructural features and with unique mechanical and physical properties.

Crystalline solids exhibit atomic or molecular structures that repeat over large atomic distances (i.e., they exhibit long-range-ordered, LRO, structures) whereas noncrystalline solids exhibit no long-range periodicity. The atomic and molecular components of both crystalline and noncrystalline solids are held together by a series of strong *primary* (i.e., ionic, covalent, and metallic) and/or weak *secondary* (i.e., hydrogen and Van der Waals) bonds. Primary bonds are usually more than an order of magnitude stronger than secondary bonds. As a result, *ceramics* and *glasses,* which have strong ionic-covalent chemical bonds, are very strong and stiff (i.e., they have large elastic moduli). They are also resistant to high temperatures and corrosion, but are brittle and prone to failure at ambient temperatures. In contrast, thermoplastic *polymers* such as polyethylene, which have weak secondary bonds between long chain molecules, exhibit low strength, low stiffness, and a susceptibility to creep at ambient temperatures. These polymers, however, tend to be extremely ductile at ambient temperatures.

In this article, some of the fundamental relationships between microstructure and mechanical properties are reviewed for the major classes of nonmetallic engineering materials. The individual topics include chemical bonding, crystal structures, and their relative influences on mechanical properties. The present article has been derived in structure and content from the article "Fundamental Structure-Property Relationships in Engineering Materials," in *Materials Selection and Design,* Volume 20 of *ASM Handbook* (Ref 2). In light of the bewildering number of different engineering materials within each class, discussions were limited to a number of general examples typifying the general features of the major classes of nonmetallic materials.

General Characteristics of Solid Materials

Engineering materials can be conveniently grouped into five broad classes: metals, ceramics and glasses, intermetallic compounds, polymers, and composite materials. Metals, ceramics and glasses, polymers, and composites represent the most widely utilized classes of engineering materials, whereas intermetallic compounds (i.e., intermetallics), which are actually subcategories of metals and ceramics, are an emerging class of monolithic materials. The general features of five major classes of materials are summarized in Fig. 1 and are described in the following sections. Though this article deals with the properties of nonmetallic materials, a brief discussion of the general characteristics of metallic materials is included where pertinent.

Metals

Metals represent the majority of the pure elements and form the basis for the majority of the structural materials. The mechanical behavior of metals depends on a combination of microstructural and macrostructural features, which ultimately depend upon bonding, chemical composition, and mode of manufacture. Metals are held together by metallic bonds. Metallic bonds arise because on an atomic scale, the outer electron shells in metals are less than half

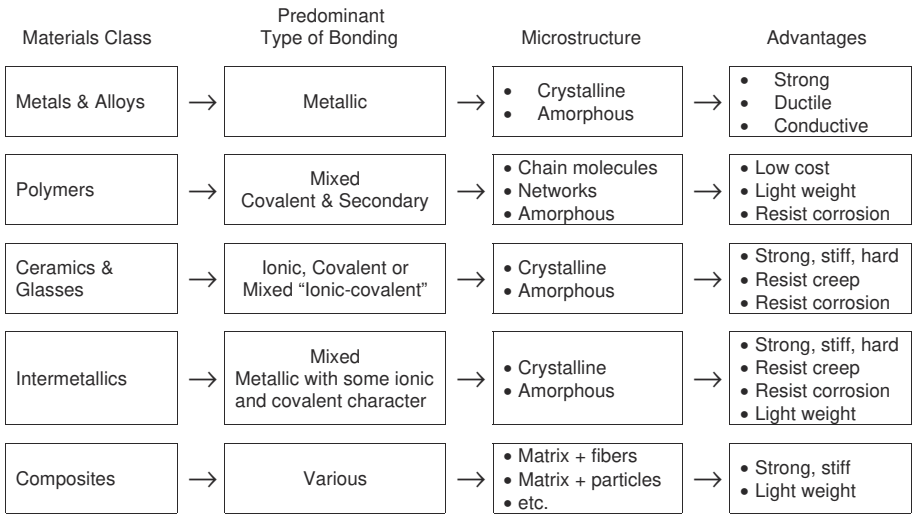

Fig. 1 General characteristics of major classes of engineering materials. Adapted from Ref 3